Journal of Power Sources 195 (2010) 232–238

Contents lists available at ScienceDirect

Journal of Power Sources

journal homepage: www.elsevier.com/locate/jpowsour

Membranes produced by plasma enhanced chemical vapor deposition technique for low temperature fuel cell applications

Aboubakr Ennajdaoui[a,b], Stéphanie Roualdes[a,*], Pascal Brault[c], Jean Durand[a]

[a] Institut Européen des Membranes, ENSCM, UM2, CNRS, Université Montpellier 2, CC 047, Place Eugène Bataillon, 34095 Montpellier cedex 5, France
[b] MID Dreux Innovation, 4 rue Albert Caquot, ZAC Porte Sud, 28500 Vernouillet, France
[c] Groupe de Recherches sur l'Energétique des Milieux Ionisés, Université d'Orléans, BP 6744, 14 rue d'Issoudun, 45067 Orléans, France

ARTICLE INFO

Article history:
Received 28 January 2009
Received in revised form 26 May 2009
Accepted 26 June 2009
Available online 7 July 2009

Keywords:
PEMFC
Plasma polymerization
Styrene
Trifluoromethane sulfonic acid
Thermal stability
Transport properties

ABSTRACT

A plasma polymerization process using a continuous glow discharge has been implemented for preparing proton conducting membranes from trifluoromethane sulfonic acid and styrene. The chemical and physical structure of plasma membranes has been investigated using FTIR and SEM. The films are homogeneous with a good adhesion on commercial gas diffusion layer (E-Tek®). Their deposition rate can be increased with increasing flow rate and input power. The thermogravimetric analysis under air of plasma polymers has showed a thermal stability up to 140 °C. Compared to the pulsed glow discharge studied in a previous paper, the continuous glow discharge has enabled to enhance the proton conductivity of membranes by a factor 3 (up to 1.7 mS cm^{-1}). Moreover, the low methanol permeability (methanol diffusion coefficient down to 5×10^{-13} m^2 s^{-1}) of membranes has been confirmed by this study. In an industrial context, a reactor prototype has been developed to manufacture by plasma processes all active layers of fuel cell cores to be integrated in original compact PEMFC or DMFC.

1. Introduction

Microfuel cells have received considerable attention over the last 10 years as a promising solution to meet the increasing demand for portable power sources for the next generation of electronics devices even smaller, lighter and more compact [1–4]. Due to their low temperature of operation, polymer electrolyte fuel cells such as PEMFC (proton exchange membrane fuel cells) and DMFC (direct methanol fuel cells) represent a large fraction of total research and development for microfuel cell applications. Studies on proton exchange membranes (PEMs) for polymer electrolyte fuel cells have especially focused on perfluorosulfonic acid membranes such as Nafion® (DuPont), Dow® (DOW Chemicals) or Flemion® (Asahi Glass) [5]. Although highly proton conductive, these membranes have several limitations such as high cost, electro-osmotic water flows and methanol crossover rates; their relatively high thicknesses limit their use in miniature devices. Therefore, much effort has been expended in developing new membranes to circumvent these disadvantages [6].

Most researchers have prepared new membranes by chemical wet process, using conventional free radical or other traditional polymerization techniques [7,8]. However, although less known than other techniques, the polymerization by plasma technology is an original method for the manufacture of competitive proton conductive membranes. Commonly referred to PECVD (plasma enhanced chemical vapor deposition), this technique offers many advantages compared to conventional polymerization processes, mainly because it introduces a high concentration of cross-links in synthesized films, favourable to high chemical and thermal stabilities [9]. Plasma polymers are dense, uniform with a good adhesion to any substrate; their thickness can be easily controlled from some nanometers up to some ten micrometers. Furthermore, plasma polymerization is a dry route method that allows the reduction of waste liquid solvents. Thus, it is cleaner and more environmentally friendly than traditional techniques.

Chemical reactions that occur under plasma conditions are generally very complex and non-specific in nature. The structure and properties of plasma polymer films depend on plasma external parameters, especially the discharge power (W), monomer flow rate (F) and pressure (P) in the reactor chamber. Plasma deposited polymers have no regular repeat unit, but consist of a random cross-linked network, which may contain some fragments of the monomer(s) structure [10,11].

For microfuel cell applications, the choice of monomers is crucial to develop the optimized plasma membrane. A number of plasma membranes have been prepared by using a mixture of two precursors in order to combine the specific properties of each of them [12–14]. Generally, one precursor is a plasma polymer-

* Corresponding author. Tel.: +33 04 67 14 91 81; fax: +33 04 67 14 91 19.
E-mail address: Stephanie.Roualdes@iemm.univ-montp2.fr (S. Roualdes).

0378-7753/$ – see front matter © 2009 Elsevier B.V. All rights reserved.
doi:10.1016/j.jpowsour.2009.06.090

izable monomer (fluorocarbons, vinylbenzene, etc.) allowing the constitution of hydrophobic backbone; the other is a functional precursor (trifluoromethane sulfonic acid, vinylphosphonic acid, water, etc.) whose role is to incorporate proton conductive groups in the polymer matrix. Many studies have shown that these plasma polymerized membranes exhibit low methanol permeability due to their highly cross-linked and dense structure; but at the expense of ionic conductivity [15].

For some years, our group have been interested in using a mixture of styrene and trifluoromethane sulfonic acid (CF_3SO_3H) monomers for preparing proton conducting electrolyte membranes by plasma polymerization. Our previous paper described the PECVD reactor and its original functionalities, in particular the impedance probe allowing a good control and reproducibility of the deposition process [16]. In this previous paper, we demonstrated that in a certain range of plasma conditions, a pulsed plasma discharge was better than a continuous plasma discharge enabling to deposit plasma polymers with a best monomers structure retention and a higher deposition rate (>100 nm min^{-1}). Nevertheless, a high limitation of the pulsed plasma discharge is the difficult priming and stability of the electric discharge out of a quite reduced range of plasma conditions (100–200 W peaking power).

In the present study, we have improved the trifluoromethane sulfonic acid injection device and investigated the plasma materials deposited in a continuous glow discharge over a large range of plasma conditions (wide modulation of power input and/or flow rates of both monomers). The physico-chemical and transport properties of plasma membranes have been investigated using different experimental methods:

- Chemical structure of plasma polymerized membranes was determined using Fourier-transform infra-red spectroscopy (FTIR).
- Thermal degradation behaviour of plasma membranes was investigated by thermogravimetric analysis (TGA) measurement.
- Morphology and thickness of plasma materials were characterized by scanning electron microscopy (SEM).
- Methanol permeability was performed using a Hittorf diffusion cell coupled to FTIR.
- Proton conductivity was measured using a mercury cell coupled to an electrochemical impedance spectroscopy device.

The objective of this research is to depict the effects of widely modulated plasma parameters on the microstructural and transport properties of plasma polymerized membranes. The impact of water immersion of plasma membranes on their physico-chemical properties will be also dealt with. Sometimes, the results will be compared to Nafion® performances.

2. Experimental/materials and methods

2.1. Preparation of membranes by plasma polymerization

All plasma membranes were prepared in a commercial capacitively coupled plasma reactor built by MHS Equipment (depicted in Fig. 1), pumped through a turbomolecular pump (ALCATEL ATH 400) for pre-deposition high vacuum and a primary pump (DVP Vacuum Technology – DC 16D) for the deposition process. The reactor is a cylindrical stainless steel chamber with the following dimensions: 600 mm long, 400 mm diameter. The pressure inside the chamber was sensed and monitored respectively by a MKS baratron gauge (626A range 0–10 mbar) and a MKS throttle valve (type 253B). A liquid nitrogen trap was placed between the deposition chamber and the pumping system in order to protect the latter. A 13.56 MHz radiofrequency (RF) source (Dressler CESAR 136) was used to supply power to the parallel and vertical plate electrodes (gap between both electrodes: 6 cm). The RF electrode is an immovable disk electrode (15 cm diameter); the grounded electrode is a rotative (speed ~6 rpm) squared electrode (15 cm × 15 cm). The substrates were placed on the grounded elec-

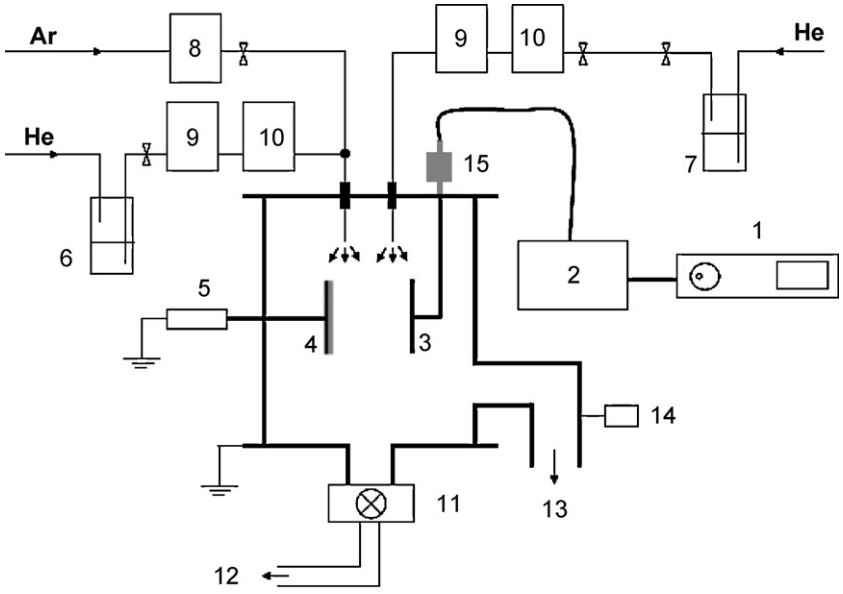

1: RF power supply	6: styrene tank	11: throttle valve
2: matchbox	7: trifluoromethanesulfonic acid bubbler	12: primary pump
3: RF electrode	8: mass flow meter	13: turbomolecular pump
4: grounded electrode (substrate holder)	9: liquid flow meters	14: capacitive gauge
5: rotating motor	10: vaporization chambers	15: impedance probe

Fig. 1. Plasma polymerization device.

Table 1
Operating conditions for the preparation of plasma polymerized membranes.

Continuous mode									
W (input power in W)	2	5	10	15	20	7	10	15	20
%F (mass flow meter opening percentage in %)	10	10	20	30	40	10	10	10	10
X parameter (W %$^{-1}$)	0.2	0.5	0.5	0.5	0.5	0.7	1.0	1.5	2.0
Process total gas pressure	0.25 mbar								
Electrodes gap	6 cm								
Argon partial pressure	0.140 mbar								
Deposition duration	2–5 h								

trode. Positioned between the generator matching network and the plasma chamber, the Z'Scan® system (Advanced Energy) was used to collect voltage, current, and phase data. This device is of great interest for the control of reproducibility and stability of the plasma discharge for long periods of deposit [16].

The glow discharge was activated by argon (Air liquid, purity >99.999%) dilution of the styrene/trifluoromethane sulfonic acid gas mixture. Argon was fed into the system via Horiba gas flow meter (SEC-E40). Styrene (Sigma Aldrich, purity >99%, liquid form) was introduced into the plasma reactor in vapor form by an appropriate injection device. The latter consists of a liquid mass flow (Horiba LF-F30MA) linked to a vaporization chamber (Horiba VC-1310), which allows a very good control of monomer flow rate (up to 0.5 g min^{-1}) without carrier gas. In the container, the polymerization of styrene monomer was stabilized by adding 15 ppm of 4-tertbutylcatechol. For transporting trifluoromethane sulfonic acid (Sigma Aldrich, purity >99%, liquid form), our previous system by argon handling [16] was abandoned in favour of the same module as for styrene injection (Horiba LF-F20MA, VC-1310 and flow rate up to 0.3 g min^{-1}). Because of its high reactivity with oxygen, trifluoromethane sulfonic acid container was prepared in a glove box, under a pure flowing nitrogen atmosphere. Both precursors were separately carried near the electrodes gap using a double pipeline gas showering system to ensure a homogeneous diffusion. All the gas lines were heated at 40 °C to prevent the polymerization/condensation of the monomers. E-Tek® carbon cloth (commercial gas diffusion layer typically used in fuel cells) with or without plasma sputtered platinum [17–19] and cleaned silicon wafers (with successively acetone, ethanol and finally dried with flowing nitrogen) were used to support plasma polymerized films. After the plasma polymerization, the reactor was evacuated by pumping, purged with argon for 10 min and then opened to the atmosphere. Silicon supported plasma films were used for microstructural characterizations (FTIR), while E-Tek® supported ones were used for methanol diffusion and proton conductivity measurements. Thermal analysis required the use of plasma materials on the form of powder which were obtained by scratching the films deposited onto silicon wafer. Concerning microstructural characterizations, a piece of each membrane deposited onto silicon wafer was post-immersed in Milliq® water for 2 h before being analyzed by SEM and FTIR.

In the plasma, the monomers are exposed to electronic bombardment which causes activation, dissociation and ionization processes. By recombination, the gas molecules fragments (radicals) form the polymer film on the substrate surface. The degree of fragmentation depends on electron density or input power, monomers flow rates and molecular weights. In order to quantify the degree of fragmentation, Yasuda and Hirotsu [20] had put forward the composite parameter $W/(F{\cdot}M)$, where W is the discharge input power (Watt or W), F is the monomer molar or volume flow rate, and M is the monomer molecular weight. $W/(F{\cdot}M)$ represents the energy supplied per unit of mass of monomer.

In the same way, we have introduced an equivalent parameter to describe the energetic character of plasma polymerization. It may be expressed by X, which is defined as:

$$X = W/(\%F) \quad (1)$$

where W is the input power (W) and $\%F$ is the opening percentage of both monomers liquid mass flow meters (%). X is expressed in W %$^{-1}$.

For all the plasma membrane depositions, the PECVD process pressure was kept constant at 0.25 mbar. In a first step, the input power was varied from 2 to 20 W and the opening percentage of each monomer liquid mass flow meter was maintained constant at 10%: X varied from 0.2 to 2 W %$^{-1}$. In a second step, at the optimal value X = 0.5 W %$^{-1}$, three kind of membranes were synthesized by multiplying simultaneously the power and the mass flow meter opening percentage by the same factor 2, 3 or 4. The plasma conditions for the preparation of membranes are summarized in Table 1.

2.2. Films thickness, morphology

The films thickness was measured by evaluating (error ∼10%) micrographs of membrane cross-sections using scanning electron microscopes (S-4500 and S-4800 Hitachi®). SEM was also used for observation of membrane surfaces and membrane/Pt/E-Tek® interfaces morphology.

2.3. Chemical structure, thermal analysis

FTIR spectra were recorded on Nicolet Impact 400D Spectrometer in the range 4000–400 cm^{-1}, 64 scans were taken on each sample with a 4 cm^{-1} resolution. In this paper, we used this technique mainly for determining the sulfonation rate *Sr* (error ∼5%) of plasma membranes immediately after the synthesis or after post-immersion in water. This parameter reflects the richness of membranes (it's not the real chemical content) in sulfonic acid groups –SO_3H. In our previous work [16], it was defined as:

$$Sr(\%) = 100 \times \frac{A_{1030}}{A_{1030} + A_{700}} \quad (2)$$

where A_{1030} is the 1030 cm^{-1} FTIR peak area (representative of sulfonic acid groups) and A_{700} the one at 700 cm^{-1} (representative of aromatic rings).

A Thermogravimetric Hi-Res 2950 (TA Instruments series) analyzer was employed to investigate the thermal stability behaviour of plasma polymer films. About 10–20 mg was heated under air atmosphere up to 1000 °C at a heating rate of 10 °C min^{-1}.

Chemical stability of plasma membranes was investigated by ex situ measuring of *Sr* (%) at different temperatures: 90, 145, 220, 300, 400 and 515 °C (reached at a heating rate of 10 °C min^{-1}). After immediate return to ambient temperature, the residual powdered samples were analyzed by attenuated total reflection FTIR analysis.

2.4. Transport properties: methanol permeability and proton conductivity

Methanol permeability was measured using a Hittorf diffusion cell. The cell was divided into two Teflon compartments clamping

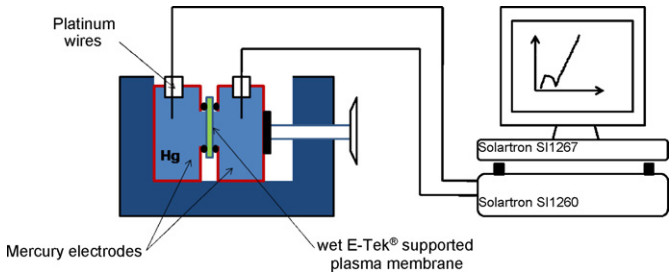

Fig. 2. Experimental device for the measurement of plasma membranes conductivity.

the membrane; one compartment was filled with Milliq® water, the other with 5 vol% methanol aqueous solution. The amount of methanol permeated through the membrane into the initially containing pure water compartment was analyzed by infrared titration.

The proton conductivity (error ~12.5%) was obtained from alternative current impedance measurements with an Solartron 1260 impedance analyzer in the frequency range 0.1 Hz–1 MHz. The mercury cell used for the measurements is depicted in Fig. 2. Before measurements, samples were dipped in H_2SO_4 (1 N) solution for 24 h at 25 °C and then rinsed in Milliq® water. More details regarding transport measurement techniques and calculations have been given in a previous communication by our group [21].

3. Results/discussions

3.1. Impedance supervision by Z'scan

A continuous monitoring of a deposition plasma procedure by the pressure control or visually is very tricky and does not enable the optimization of the duration of each sequence at the beginning of the procedure. Indeed, after the styrene injection for example, the induced variation of the throttle valve opening percentage is not very perceptible and the change of plasma phase composition is hardly appreciable by eyes. The Z'scan probe can provide a solution to this limitation.

Positioned at the output of the matching box, the Z'scan device measures real voltage, real current and real phase shift between voltage and current at the point of measurement [16]. All other plasma parameters like the delivered power or impedance can be calculated from these three values. The supervision in real time of a deposition plasma procedure by the measurement of plasma impedance is very performing. Indeed, each sequence in the procedure (such as a precursor's injection) which leads to a plasma parameter variation (such as total pressure gas or monomer flow rates) translates into a perceptible plasma impedance variation. Thus, the Z'scan probe can be a judicious device to reduce the duration of some sequences at the beginning of a plasma deposition procedure and ensure its good running.

Fig. 3 shows the plasma impedance evolution as a function of time for two different plasma sequences A and B. In both sequences, the start of the plasma impedance recording ($t = 0$) corresponds to the start of the argon plasma. Preliminary studies have shown that the decreasing trend of the impedance for the first 1000 s is directly related to the cleaning of the reactor walls (etching of the previous deposits). In the sequence A, both precursors are injected in the same time at $t = 1000$ s, once the reactor walls being considered as clean. In the sequence B, in accordance with that implemented in this study for the preparation of membranes, styrene is the first injected at $t = 1100$ s and then trifluoromethane sulfonic acid at $t = 1850$ s. For the sequence A, the plasma impedance variations show that the time for a steady-state dilution of both monomers inside the argon plasma after injection (translated into the stabilization of the plasma impedance) is about 600 s. For the sequence B, the plasma impedance variations show that the time for a steady-state dilution of styrene inside the argon plasma after injection is about 300 s; while only 150 s is necessary for the dilution of trifluoromethanesulfonic acid which is much more fluid. Once the plasma impedance stabilized, the membrane deposition really begins. Z'scan supervision is especially useful for the sequence B (favoured in this study) where we can easily anticipate the injection of trifluoromethane sulfonic acid knowing the time for plasma styrene stabilization, thus saving time.

3.2. Morphologies and deposition rates

Fig. 4 shows SEM profiles of a typical sulfonated polystyrene-type plasma polymerized membrane deposited onto platinized

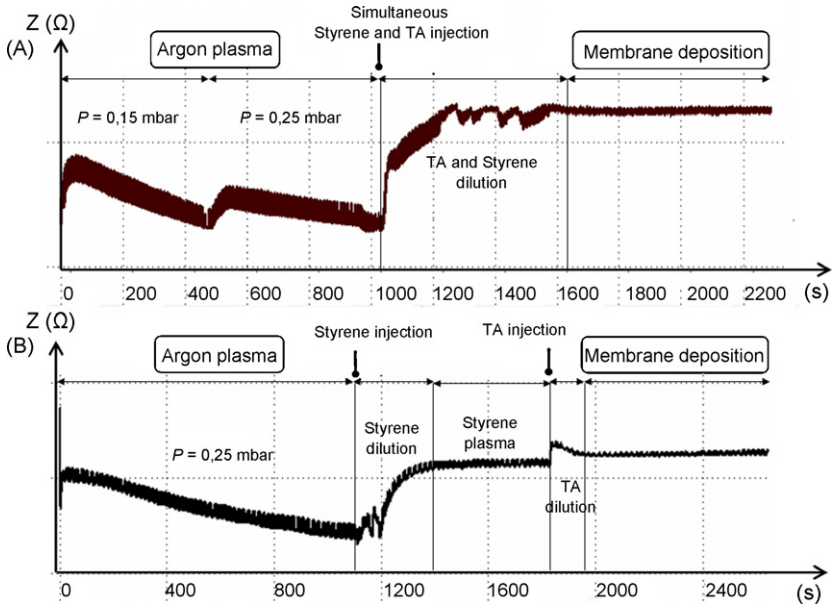

Fig. 3. Plasma impedance (Z) measurement of plasma for two different plasma sequences A (simultaneous injection of precursors) and B (delayed injection) to start the membrane deposition (TA: trifluoromethane sulfonic acid; P: total pressure).

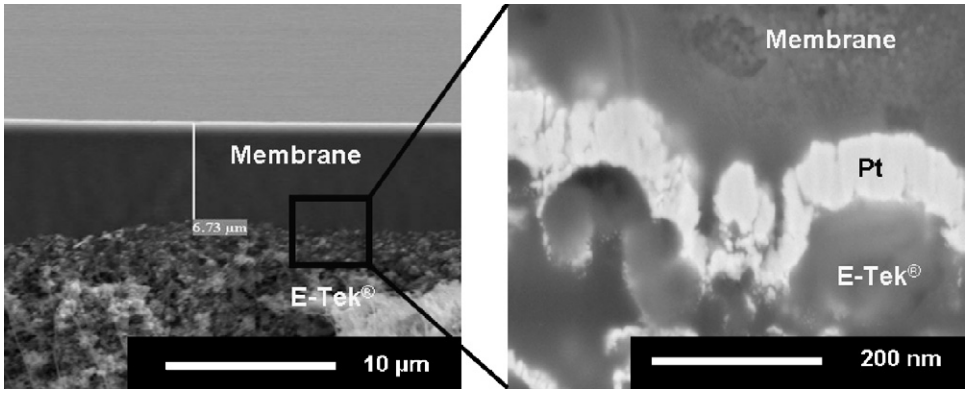

Fig. 4. SEM profiles of a plasma membrane on platinized E-Tek® gas diffusion layer (S-4500 Hitachi®); on the right magnification of the membrane/Pt/E-Tek® interface (sample preparation by cross polisher, SEM observation with S-4800 Hitachi®).

E-Tek® support. Even if the platinized E-Tek® carbon cloth is very rough and porous (20%), the plasma membrane is dense, flat, uniform, free from defects and perfectly adherent on its support. A magnification of the membrane/Pt/E-Tek® interface allows to see the membrane diffusion across the platinized carbon support [17]. This predicts a good quality of the triple point between fuel, catalyst (Pt) and membrane required for good fuel cells performance.

Depending on deposition duration and plasma parameters, deposited polymer films exhibit a thickness in the 5–30 μm range. Fig. 5 exhibits the growth kinetics of the plasma polymers deposited at different *X* values. In the case of constant *%F* equal to 10% and variable *W*, the deposition rate *R* increases with the *X* parameter in the range 0.2–0.7 W%$^{-1}$ and then keeps quite constant for higher values of *X* (note that it is not interesting to consider the *R* at 2.0 W%$^{-1}$ because of powder formation under these plasma conditions. Such observed phenomenon is not understood yet, but is certainly related to specific species density and nature in the plasma chamber). This evolution has been described by Yasuda as the Competitive Ablation and Polymerization (CAP) principle [22]: slightly energetic plasmas (relative to *X* values lower than 0.7 W%$^{-1}$ here) refer to the energy deficient region where an increase of the input power induces an increase of the number of monomer fragments and thus, the enhancement of the deposition rate; whereas highly energetic plasmas (relative to *X* values higher than 0.7 W%$^{-1}$ here) refer to the monomer deficient region where an increase of the input power does not enable the formation of further fragments making the deposition rate keeping constant.

The optimum deposition rate (155 nm min^{-1}) is found at the frontier between both regions (*X* = 0.7 W%$^{-1}$). At 0.5 W%$^{-1}$, by multiplying *W* and *%F* by an identical factor 2, 3 or 4, the deposition rate increases from 120 up to 160, 240 or 320 nm min^{-1}, respectively, under the effect of an increased amount of supplied monomer fragments. These deposition rates are higher than those (120 nm min^{-1}) obtained under pulsed plasma configuration in our previous research [16]. After soaking in Milliq® water for 2 h, it was observed by SEM a decrease of membrane thicknesses. Depending on plasma conditions, this decrease represents between 10 and 20% of the total thickness. This observation has already been explained by the condensation of trifluoromethane sulfonic acid molecules on the support surface when the plasma polymerization is turned off [15]. This condensation thin layer on the membrane surface disappears after water immersion.

3.3. Sulfonation rates

Fig. 6 presents the effect of the *X* parameter on the sulfonation rate *Sr* deduced from FTIR spectra and representative of the $-SO_3H$ content in membranes. Two regions can be distinguished. For *X* values lower than 0.5 W%$^{-1}$ (*%F* = 10%), the sulfonation rate increases from 35 up to 65% with *X*. Above 0.5 W%$^{-1}$ (optimum), it decreases from 65 down to 52%. That can be explained by the increase of the number of $-SO_3H$ fragments incorporated in films in the energy deficient region and the decomposition of $-SO_3H$ moieties into smaller fragments in the monomer deficient region. Moreover, the sulfonation rate only slightly decreases (from 65 to 62%) by multiplying *W* and *%F* at 0.5 W%$^{-1}$. This not very pronounced variation proves that the chemical structure of membranes

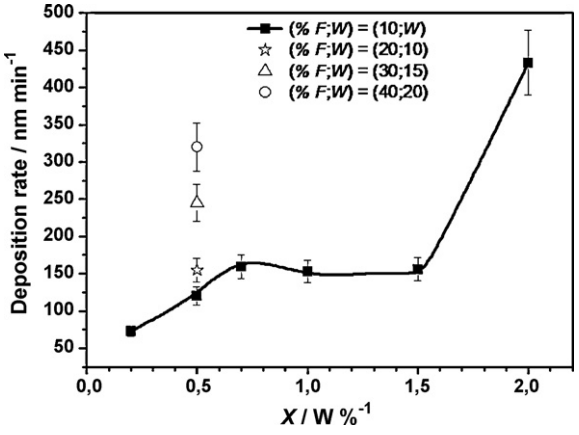

Fig. 5. Deposition rate *R* versus the *X* parameter for different (*%F*;*W*) values.

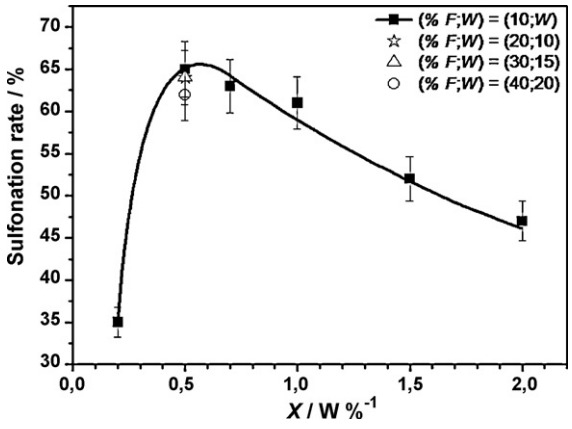

Fig. 6. Sulfonation rate versus the *X* parameter for different (*%F*;*W*) values.

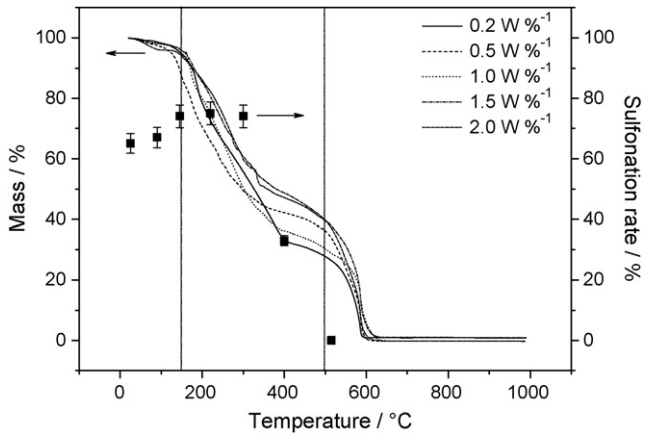

Fig. 7. Thermogravimetric curves of plasma membranes deposited at different X values. For the membrane deposited at $X = 0.5\ W\%^{-1}$: sulfonation rate Sr at ambient temperature (25 °C) and after heating at 90, 145, 220, 300, 400 and 515 °C.

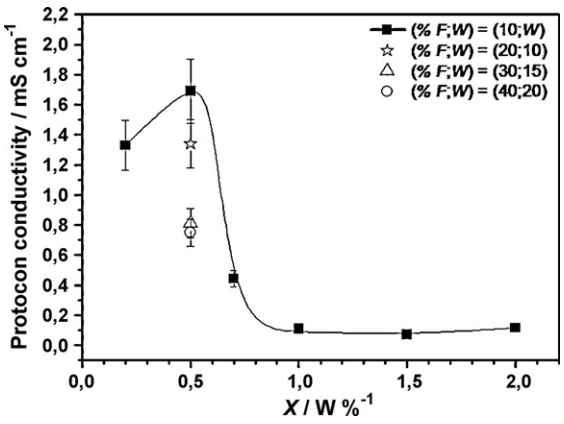

Fig. 8. Proton conductivity versus the X parameter for different (%F;W) values.

is directly related to the monomer fragmentation rate (given by X) and quasi-independent on the amount of supplied monomer fragments.

The elimination (previously observed by SEM) of the upper condensated sulfonated layer on the membrane after water immersion was confirmed by the decrease of sulfonation rate values by 50%.

3.4. Thermal stability

Fig. 7 shows the thermogravimetric curves for five kinds of membranes synthesized at different X values: 0.2, 0.5, 1.0, 1.5, and 2.0 $W\%^{-1}$, over the temperature range 25–1000 °C. On the left, the y-axis represents the sample mass in % and on the right the sulfonation rate of the membrane deposited at $X = 0.5\ W\%^{-1}$ after heating at different temperatures. It was considered that initial thermal degradation starts at 5% in mass loss; $T_{d5\%}$ is referred to the temperature for that specific mass loss.

Whatever the plasma membranes investigated, there are two distinct stages of decomposition: the first step occurs around 150 °C and the second around 500 °C. Concerning the first step of degradation, it was observed for all the membranes a loss of about 60% in weight whose origin has not been eluded. The membrane deposited at $X = 0.5\ W\%^{-1}$ conditions who exhibits the highest sulfonation rate ($Sr = 65\%$), has the lowest $T_{d5\%}$ equal to 143 °C. In contrast, the membrane synthesized at $0.2\ W\%^{-1}$ and with the least sulfonic acid groups content ($Sr = 35\%$) began to deteriorate at a temperature of 189 °C. It can be seen from above results that membrane thermal stability decreases as the sulfonation rate increases. Directly related to the presence of $-SO_3H$ groups, the membrane thermal stabilities are weakened [23].

After 500 °C, the second step of thermal degradation can be attributed to the complete decomposition of the polymer carbonaceous matrix [24].

Anyway, temperatures from which the membranes begin their degradation (143 °C) remain high enough to make them withstand the PEMFC's operating temperature (around 80 °C).

The evolution of sulfonation rate versus the temperature of the heating post-treatment is also shown in Fig. 7 for one plasma membrane ($X = 0.5\ W\%^{-1}$). Up to 300 °C, the sulfonation rate increases from 65 to 75%, which can be attributed to the combination of two phenomena: the volatilization of carbon chain fragments and oxidation of $-SO_2$ sites into $-SO_3-$ groups. Above 300 °C, the membrane desulfonation occurred with a reduction of more than half of sulfonation rate at 400 °C ($Sr = 33\%$); then at 515 °C, the loss of SO_3–H groups becomes total ($Sr = 0\%$).

3.5. Transport properties

3.5.1. Proton conductivity

The evolution of the proton conductivity versus X is plotted in Fig. 8 for membranes deposited in different (%F;W) plasma conditions. The membranes synthesized at 0.2 and $0.5\ W\%^{-1}$ possess the highest proton conductivities equal to 1.33 and 1.69 mS cm^{-1}, respectively. These values are 3–4 times higher than the proton conductivities measured for layers deposited in pulsed plasma configuration [16]. At $0.5\ W\%^{-1}$, although the sulfonation rate does not really change by multiplying W and %F, the proton conductivity is clearly affected (from 1.69 down to 0.75 mS cm^{-1}). Above $0.5\ W\%^{-1}$, for which the proton conductivity reaches a maximum, a further increase of X produces a drop in the proton conductivity because of enhanced fragmentation of sulfonic acid groups in the plasma and increased cross-linking degree of the polymers.

We have also noticed that the membrane conductivities are not only dependent on their sulfonation rates. Indeed, the membrane sulfonation rates at $0.5\ W\%^{-1}$ and $1.0\ W\%^{-1}$ are equivalent; and yet, the difference in their proton conduction ability is of a factor 10. This result shows that the $-SO_3H$ group content is not the only structural parameter having an influence on the proton conductivity. On that subject, it is well known that the density of plasma membranes plays an important role in the membrane transport properties. Above $0.5\ W\%^{-1}$, we can suppose that plasma polymerized films formed are too dense to provide sufficient water and proton mobility.

Precisely due to their highly cross-linked structure, the proton conductivity of plasma membranes are lower than that of Nafion® 117 (70 mS cm^{-1} in the same experimental conditions). Indeed, $-SO_3H$ groups in Nafion® are aggregated on the form of transport channels providing good performance in ionic conductivity. While the sulfonic acid groups in plasma polymers are randomly dispersed through the disorganized structure of membranes, hence reducing the proton mobility. Nevertheless comparable level conduction (specific resistance) to Nafion® can be obtained for very thin plasma membranes for which thickness is tunable by plasma polymerization duration down to some micrometer thickness. Indeed, a 4.5 μm thick plasma membrane synthesized at $X = 0.5\ W\%^{-1}$ (1.69 mS cm^{-1}) has the same specific resistance (0.26 Ω cm^2) as Nafion® 117.

3.5.2. Methanol diffusion permeability

As reported in Table 2, plasma membranes are characterized by diffusion coefficients between 5.1×10^{-13} and 15.9×10^{-13} m^2 s^{-1} (except at $0.2\ W\%^{-1}$ for which the very high diffusion coefficient equal to 117×10^{-13} m^2 s^{-1} is directly related to the powdered nature of the film). So they are intrinsically 85–270

Table 2
Methanol (5 vol% dilution) permeability measurements of plasma membranes deposited at various *X* parameters (comparison with Nafion® 117).

X (W %$^{-1}$)	Methanol diffusion coefficient D ($\times 10^{-13}$ m^2 s^{-1})	Methanol flux J ($\times 10^{-5}$ mol m^{-2} s^{-1})
0.2	8.4	4.1
0.5	6.6	2.3
1.0	15.9	4.3
1.5	5.1	1.3
2.0	117	1.6
Nafion® 117	1370	91

times less permeable to methanol than Nafion® 117 membrane (1370×10^{-13} m^2 s^{-1}). This is due to their high density and highly cross-linked three-dimensional structure [18]. Concerning the methanol flux (extrinsic property), the deviations between plasma membranes and Nafion® are less important because of significant differences in thicknesses between the two kinds of membranes (185 μm for Nafion® 117 and up to 30 μm for plasma membranes); nevertheless the characteristic methanol flux of plasma membranes remain much below than that of Nafion® membrane. Thus, the use of plasma membranes of a few microns (5–30 μm) thicknesses in microfuel cells is very interesting because it can allow a reduction of methanol crossover by a factor 22–70 compared to Nafion® 117. The surprising evolution of the methanol permeability as a function of the *X* parameter is not elucidated yet; it is certainly related to joint effects of chemical composition and density of plasma films (still under investigation).

4. Conclusion

Sulfonated polystyrene-type membranes have been prepared by plasma polymerization in a continuous plasma discharge under different operating conditions. The benefits of the Z'scan device for the optimization (in particular time reduction) of the plasma deposition procedure has been demonstrated. The monomers flow rate and discharge input power variations have enabled to distinguish two plasma operating regions (deficient in monomer or in input power) according to the CAP principle proposed by Yasuda. The results obtained in our previous work on morphology (flat, uniform, good compatibility) and methanol permeability (much lower than that of Nafion®) of plasma membranes synthesized in a pulsed plasma discharge are the same here in the case of a continuous plasma discharge. In continuous mode and thanks to a better control of the injection of trifluoromethane sulfonic acid, our study allows improving significantly some membranes properties. Indeed, an optimized proton conductivity of 1.69 mS cm^{-1} has been obtained; the deposition rate could be increased up to 320 nm min^{-1} without really affecting membranes microstructural properties. The thermal stability measurements have shown that plasma membranes easily support the operating temperature of PEMFC or DMFC; those containing few SO_3–H groups are the most stable, unfortunately to the detriment of proton conductivity.

Taking into account those good features, original MEAs (membrane electrode assemblies) were manufactured by plasma processes in order to develop thick compact (~1 mm) fuel cell cores. Recently, MEAs' integration was improved using a linear industrial prototype which combines plasma polymerization for the membrane deposition and plasma sputtering for Pt deposition in a single device. First plasma fuel cell preparations on such an industrial device are in progress.

Acknowledgements

MID Dreux Innovation, MHS Equipment, ESF-European Union, French Ministry of Research, Région Centre and CNRS are acknowledged for granting this work. The authors are very grateful to MHS Equipment for providing plasma reactors and Didier Cot from the Institut Européen des Membranes for performing SEM analyses.

References

[1] J.D. Morse, Int. J. Energy Res. 31 (2007) 576–602.
[2] D.-E. Park, T. Kim, S. Kwon, C.-K. Kim, E. Yoon, Sens. Actuators A 135 (2007) 58–66.
[3] N. Wan, C. Wang, Z. Mao, Electrochem. Commun. 9 (2007) 511–516.
[4] J. Yeom, G.Z. Mozsgai, B.R. Flachsbart, E.R. Choban, A. Asthana, M.A. Shannon, P.J.A. Kenis, Sens. Actuators B 107 (2005) 882–991.
[5] B. Smith, S. Sridhar, A.A. Khan, J. Membr. Sci. 259 (2005) 10–26.
[6] M.A. Hickner, H. Ghassemi, Y.S. Kim, B.R. Einsla, J.E. McGrath, Chem. Rev. 104 (2004) 4587–4612.
[7] R.K. Nagarale, G.S. Gohil, V.K. Shahi, Adv. Colloid Interface Sci. 119 (2006) 97–130.
[8] R.-Q. Fu, J.-J. Woo, S.-J. Seo, J.-S. Lee, S.-H. Moon, J. Membr. Sci. 309 (2007) 156–164.
[9] I.-S. Bae, S.-H. Cho, S.-B. Lee, Y. Kim, J.-H. Boo, Surf. Coat. Technol. 193 (2005) 142–146.
[10] H. Yasuda, Plasma Polymerization, Academic Press, Orlando, FL, 1985.
[11] R. D'agostino, Plasma Deposition, Treatment, and Etching of Polymers, Academic Press, 1990.
[12] L. Mex, J. Müller, Membr. Technol. 115 (1999) 5–9.
[13] L. Mex, N. Ponnat, J. Müller, Fuel Cell Bull. 39 (2001) 9–12.
[14] L. Mex, M. Sussiek, J. Müller, Chem. Eng. Commun. 190 (2003) 1085–1095.
[15] H. Mahdjoub, S. Roualdès, P. Sistat, N. Pradeilles, J. Durand, G. Pourcelly, Fuel Cells 5 (2005) 277–286.
[16] A. Ennajdaoui, J. Larrieu, S. Roualdès, J. Durand, Eur. Phys. J. Appl. Phys. 42 (2008) 9–16.
[17] A. Caillard, P. Brault, J. Mathias, C. Charles, R.W. Boswell, T. Sauvage, Surf. Coat. Technol. 200 (2005) 391–394.
[18] H. Rabat, P. Brault, Fuel Cells 8 (2008) 81–86.
[19] A. Caillard, C. Coutanceau, P. Brault, J. Mathias, J.-M. Léger, J. Power Sources 162 (2006) 66–73.
[20] H. Yasuda, T. Hirotsu, J. Polym. Sci., Polym. Chem. Ed. 16 (1978) 743–759.
[21] S. Roualdes, I. Topala, H. Mahdjoub, V. Rouessac, P. Sistat, J. Durand, J. Power Sources 158 (2006) 1270–1281.
[22] H.K. Yasuda, Plasma Polymerization and Plasma Interactions with Polymeric Materials, John Wiley & Sons, New York, 1990.
[23] M.-H. Yang, Polym. Degrad. Stab. 76 (2002) 69–77.
[24] Z. Wang, X. Li, C. Zhao, H. Ni, H. Na, J. Power Sources 160 (2006) 969–976.